Pathology International

*Pathology International* 2011; **61**: 67–72 doi:10.1111/j.1440-1827.2010.02615.x

Original Article

# Combined expression of miR-122a, miR-1, and miR-200b can differentiate degraded RNA samples from liver, pancreas, and stomach

**Joseph Kim, Na Eun Choi, Su Jin Oh, Sang Jae Park and Hark Kyun Kim**

*National Cancer Center, Goyang, Republic of Korea*

**The effect of RNA degradation on the diagnostic utility of microRNA has not been systematically evaluated in clinical samples. We asked if the microRNA profile is preserved in degraded RNA samples derived from mouse and human tissue. We selected tissue-specific microRNA candidates from published human microarray data, and validated them using quantitative reverse transcription polymerase chain reaction (QRTPCR) analyses on flash-frozen, normal mouse liver, pancreas, and stomach tissue samples. MiR-122a, miR-1, and miR-200b were identified as tissue-specific, and the 3-microRNA-based QRTPCR could predict the tissue origin for mouse tissue samples that were left at room temperature for 2 h with an accuracy of 91.7%. When we applied this 3-microRNA predictor to clinical specimens with various degree of RNA degradation, the predictor differentiated degraded RNA samples from liver, pancreas, and stomach with an accuracy of 90% (26/29). Expression levels of miR-122a, miR-1, and miR-200b were modestly changed after the extended (2–4 h) storage at room temperature, but the magnitudes of expression changes were small compared to the expression differences between various tissues of origin. This proof-of-principle study demonstrates that RNA degradation due to extended storage at room temperature does not affect the predictive power of tissue-specific microRNA QRTPCR predictor.**

**Key words:** microRNA, RNA degradation, specific, tissue

## INTRODUCTION

MicroRNAs are evolutionarily-conserved, RNA molecules of 19–22 nucleotides, and can function as potential oncogenes or tumor suppressor genes, depending on the cellular context and the target genes.[1,2] Accumulating evidence suggests the potential utility of microRNA as diagnostic aids or therapeutic targets.[1] One problem in developing RNA-based diagnostic tools is that RNA is easily degraded when it is isolated from RNase-rich tissue samples, such as the pancreas or gastrointestinal tract. Ischemic time of resected samples may sometimes be extended up to an hour or two, resulting in the RNA degradation. The stability of microRNA in such degraded RNA samples is under active investigation, but not clearly understood.[3,4] Xi *et al*. reported that the expression profiles of microRNAs were in good correlation between fresh frozen and formalin-fixed, paraffin-embedded (FFPE) samples ($R^2$ = 0.86–0.89),[5] suggesting the relative stability of microRNA in clinical samples with poor RNA quality. Thus, it seems that microRNAs are less susceptible to degradation than the longer mRNAs, but the stability of microRNAs in tissue samples in which RNAs have been degraded due to extended storage at room temperature has not been systematically evaluated in clinical tissue specimens.

One of the most important clinical uses of microRNA profiling of cancer tissue samples is its ability to predict the tissue origin of metastasis.[6] MicroRNA is crucial to development and is known to be tissue-specific.[7] Several investigators have suggested that monitoring microRNA expression profile may be a feasible approach to the diagnosis of primary tissue origin.[6] To address the question of whether the microRNA profile is preserved in tissue samples with degraded RNA, we tested the predictive power of a set of tissue-specific microRNA in clinical samples of various RNA qualities. We selected tissue-specific microRNAs by performing microRNA quantitative real-time reverse

Correspondence: Sang Jae Park, MD, PhD, Head, Center for Liver Cancer, National Cancer Center, Goyang, Republic of Korea, 410-769. Email: spark@ncc.re.kr or Hark Kyun Kim, MD, PhD, Senior Scientist, Cancer Cell and Molecular Biology Branch, National Cancer Center, Goyang, Republic of Korea, 410-769. Email: hkim@ncc.re.kr

Received 24 August 2010. Accepted for publication 6 October 2010.

transcription polymerase chain reaction (QRTPCR) on flash-frozen tissue samples derived from mouse liver, pancreas, and glandular stomach. These three organs develop from the same foregut endoderm[8] and may have relatively similar microRNA expression profiles. In addition, these are among most common primary cancer organ sites in Japan and Korea. Pancreatic and gastric cancers often metastasize to the liver, sometimes as sole lesions. In these cases, it becomes important to differentiate between primary and metastatic cancers in the liver.

Here we report that tissue-specific microRNAs identified using mouse flash-frozen samples can differentiate degraded RNA samples from liver, pancreas, and stomach with a high accuracy. This proof-of-concept study demonstrates that degraded RNA samples from liver, pancreas, and stomach can be used for tissue origin prediction using QRTPCR for miR-122a, miR-1, and miR-200b.

## MATERIALS AND METHODS

### RNA preparation

Liver, pancreas, and glandular stomach tissues were procured from severe combined immunodeficiency (NOD/SCID) mice aged 5–10 weeks under isoflurane anaesthesia. Liver, pancreas, and glandular stomach tissue samples were either rapidly frozen in nitrogen immediately after resection ($n = 4$ mice; *flash-frozen*/*0-h*, hereafter), left at room-temperature for 2 h ($n = 4$; *2-h,* hereafter), or formalin-fixed and paraffin-embedded (FFPE, $n = 4$). While there are various experimental methods for degrading RNA, such as exposure to high temperature[4] or UV light,[9] we intended to introduce RNA degradation by mimicking clinical situations. Hence, fresh tissue organs were wrapped in aluminium foil and left at room temperature for 2 h.

We also used 29 total RNA samples which were collected from 16 patients with cancers originating from liver, pancreas, distal common bile duct, or stomach. Informed consents for the use of tissue samples in genetics research were signed by these patients. The median age of patients was 48 years (interquantile range, 56–66) with 7 (43.8%) males. Nineteen of the 29 clinical samples were surgically collected either from cancer lesions or from adjacent benign lesions (Table 3). Surgical tissue samples were rapidly frozen in liquid nitrogen within 30 min of procurement (*flash-frozen* or *0-h*, hereafter), left at room temperature for 2 h longer than flash-frozen samples as described above for mouse samples (*2-h,* hereafter), or incubated at room temperature for 4 h longer than flash-frozen samples (*4-h,* hereafter). Ten of 29 clinical samples were derived from endoscopic biopsy tissue collected from gastric cancer patients. These endoscopic biopsy samples were once thawed while they were processed for a proteomics study[10] and considered to have degraded RNA. Frozen tissue samples were mechanically crushed in liquid nitrogen, homogenized, and subject to RNA isolation using TRI reagent (Invitrogen, Carlsbad, CA, USA) according to the manufacturer's instructions. RNA was isolated from FFPE samples using MasterPure kit (Epicentre Biotechnologies, Madison, WI, USA). The concentrations of isolated total RNA samples were determined using the NanoDrop ND100 (NanoDrop Technologies, Wilmington, DE, USA). The average $A_{260}/A_{280}$ ratio for all of the 65 RNA samples analyzed in this study was $1.9 \pm 0.2$ (Mean $\pm$ SD). The 2100 Bioanalyzer (Agilent Technologies, Santa Clara, CA, USA) was used to evaluate the RNA integrity. RNA integrity number (RIN) is calculated by the instrument software to simplify the assessment of RNA integrity.[11] A RIN of 1 represents almost fragmented and degraded RNA and a RIN of 10 represents intact and non-fragmented RNA. A previous report demonstrated that RIN is better correlated with the QRTPCR expression of the house-keeping genes than is the 28S/18S ribosomal ratio.[11]

### microRNA quantitative RT-PCR (QRTPCR)

Candidate tissue-specific microRNAs for subsequent QRTPCR analyses were chosen from the published data from a human study.[7] Published microarray data were downloaded from Broad Institute website (http://www.broadinstitute.org/cgi-bin/cancer/datasets.cgi) and expression levels were thresholded at 500. MicroRNAs that were differentially expressed according to the data from human liver, pancreas, and stomach tissue samples were selected based on analysis of variance (ANOVA) at $P$ cut-off level of 0.01. RNA samples isolated from mouse flash-frozen tissue samples were first subjected to QRTPCR analyses for 12 candidate microRNAs selected from published human data (Table 1). Cycle threshold ($C_t$) value of each microRNA was normalized to RNU6 by subtraction. The average expression level of the 12 microRNAs in each normal mouse organ was correlated to that of the published human microarray data, and microRNAs with Pearson correlation $> 0.9$ were selected for subsequent analyses (Table 1). Overlapping tissue-specific microRNAs were identified, and monitored for expression in degraded RNA samples from normal mouse organs. DNAse I (QIAGEN, Valencia, CA, USA) -treated total RNA (1 microgram) was used for reverse transcription, and 5% of the reverse transcription product was used for real-time PCR. The miScript PCR system (QIAGEN) was used for QRTPCR. Each QRTPCR reaction was performed in duplicate reactions in a 96-well plate, using a LightCycler 480 Instrument II (Roche, Basel, Switzerland). Annealing temperatures were set at

**Table 1** QRTPCR analyses on flash-frozen normal NOD/SCID mouse organs using candidate tissue-specific microRNAs adopted from published human microarray data

| | Normalized $C_t$† (Mean ± SD) | | | |
|---|---|---|---|---|
| microRNA‡ | Liver | Pancreas | Stomach | Correlation§ |
| Hmr_miR-122a | 1.1 ± 0.9 | 14.8 ± 5.3 | 8.3 ± 1.7 | 0.998 |
| Hm_miR-1 | 14.9 ± 2.9 | 15.7 ± 2.5 | 10.5 ± 3.1 | 0.993 |
| Hmr_miR-21 | 5.0 ± 1.9 | 7.4 ± 1.5 | 5.8 ± 2.6 | –0.998 |
| Hmr_miR-143 | 12.2 ± 3.1 | 12.1 ± 2.7 | 6.8 ± 2.4 | 0.814 |
| Hmr_miR-214 | 13.2 ± 0.4 | 11.6 ± 0.6 | 11.4 ± 0.9 | 0.442 |
| Hmr_miR-181a | 11.1 ± 0.3 | 8.3 ± 0.6 | 8.4 ± 0.4 | 0.475 |
| Hm_miR-199a* | 5.2 ± 1.7 | 7.0 ± 3.5 | 2.7 ± 3.5 | –0.211 |
| Hmr_miR-23a | 5.0 ± 2.8 | 4.6 ± 0.6 | 4.2 ± 0.4 | 0.513 |
| Hmr_miR-181c | 14.1 ± 0.4 | 11.4 ± 0.6 | 11.1 ± 0.5 | 0.423 |
| Hmr_miR-125a | 7.1 ± 3.0 | 5.0 ± 1.7 | 6.2 ± 0.6 | 0.786 |
| Hmr_miR-221 | 8.5 ± 1.8 | 10.4 ± 0.8 | 9.9 ± 0.8 | –0.750 |
| Hm_miR-200b | 12.0 ± 0.5 | 9.0 ± 0.5 | 8.3 ± 0.7 | 0.983 |

†Normalized $C_t$ = $C_t$ of a given microRNA – $C_t$ for RNU6.

‡Sorted according to the ascending order of ANOVA *P* value for feature selection based on published microarray data.

§Pearson correlation coefficient between the mean QRTPCR expression (20-normalized Ct) of each organ with mean signal value in the published microarray data.

ANOVA, Analysis of variance; $C_t$, Cycle threshold; QRTPCR, Quantitative Reverse Transcription Polymerase Chain Reaction; SCID, Severe Combined Immunodeficiency; miR-199a*, miR-199 star strand.

50°C for miR-122a, miR-1, and miR-200b and at 55°C for RNU6.

### Statistical analysis

BRB-Arraytools (version 3.8, NCI)[12] was used for unsupervised and supervised analyses. QRTPCR $C_t$ data were first normalized for RNU6 as described above, and (20-normalized $C_t$ value) was used as the QRTPCR microRNA expression level. Hierarchical clustering and principal component analyses were performed using 1-correlation as a distance metric. Class prediction analyses were performed on flash-frozen, normal NOD/SCID mouse liver ($n$ = 4), pancreas ($n$ = 4), and stomach tissues ($n$ = 4) as a training set. Leave-one-out cross validation was performed for the training set using linear discriminant analysis, 1-nearest neighbor, 3-nearest neighbors, and nearest centroid predictors, which are offered by BRB-ArrayTools. The best of these four predictors, which was selected for having the lowest misclassification rate in the training set, was nearest centroid in this study. This algorithm was used to predict the class label of the following three test sets; the same mouse tissue samples either left at room temperature for 2 h ($n$ = 12) or formalin-fixed ($n$ = 12), and clinical tissue samples ($n$ = 29). In the nearest centroid algorithm, the centroid of each class (*i.e.* liver, pancreas, or stomach) is defined as a vector containing the average QRTPCR microRNA expression level of the training samples in each class[12] (User's manual, BRB-ArrayTools version 3.8). There is a component of the centroid vector for each tissue-specific microRNA. The distance of the microRNA expression profile for the test sample to each of the three centroids is measured and the test sample is predicted to belong to the class corresponding to the nearest centroid.

## RESULTS

To select evolutionarily-conserved, tissue-specific microRNAs that can be used for the current study, we downloaded published human microRNA microarray data. From the published microarray data, we identified microRNAs that are differentially expressed in liver, pancreas, and stomach tissue samples at a feature selection $P$-value < 0.01. Next, we performed QRTPCR on these microRNAs using total RNA samples isolated from flash-frozen, normal mouse organs (Fig. 1a). Average expression level of respective microRNAs in each normal mouse organ was correlated with that of published human microarray data, and microRNAs with Pearson correlation > 0.9 were identified (Table 1). Leave-one-out cross validation was performed on flash-frozen normal mouse organ RNA samples using these three tissue-specific microRNAs—miR-122a, and miR-1, and miR-200b. Of predictive algorithms used (linear discriminant analysis, 1-nearest neighbor, 3-nearest neighbors, and nearest centroid algorithms), nearest centroid gave the lowest misclassification rate of 8%. Hence, all subsequent class prediction analyses were performed using nearest centroid predictor.

The three microRNAs were evaluated using QRTPCR for normal mouse organs that were left at room temperature for 2 h and that were fixed in formalin. RNA samples isolated from pancreatic tissues that were left at room temperature for 2 h were found to be degraded, with significantly lower RNA integrity number (RINs) than flash-frozen pancreas samples (Student $t$-test $P$ = 0.002; Mean RIN ± SD, 6.0 ± 0.9 (0-h)

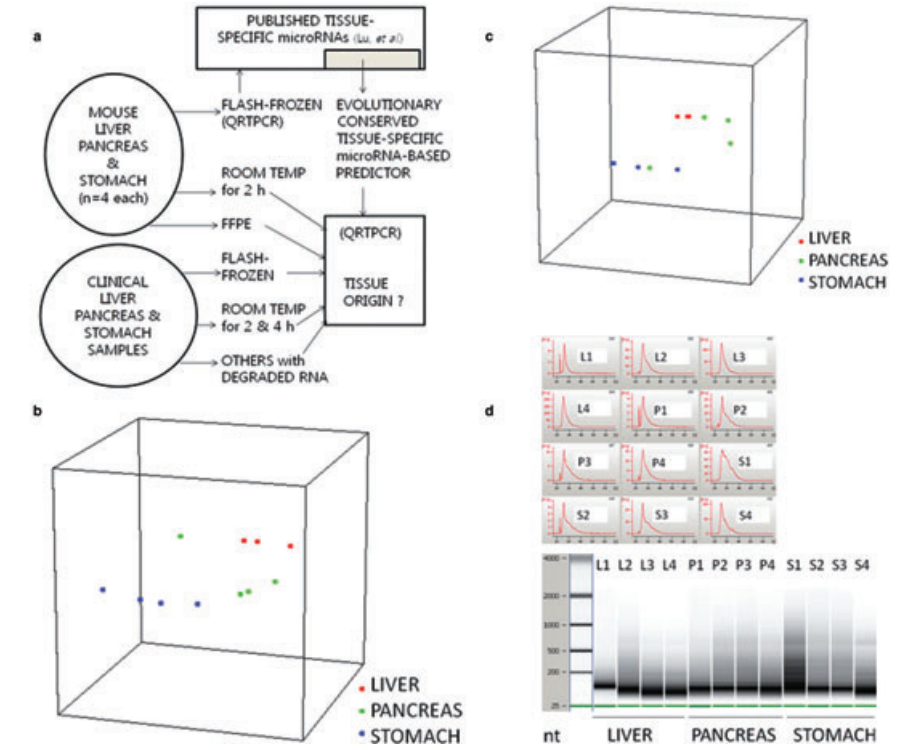


**Figure 1** (**a**) Study scheme. (**b**) A principal component analysis (PCA) plot for mouse normal organs that were left at room temperature for 2 h, based on the expression of miR-122a, miR-1, and miR-200b. Each sphere represents a RNA sample, and samples with similar microRNA profiles are located close together (distance metric, 1-correlation). The 2-h RNA samples from normal mouse liver, pancreas, and stomach tissues tended to be clustered according to their tissue origin. (**c**) A PCA plot for formalin-fixed, paraffin-embedded (FFPE) mouse normal organs based on the expression of miR-122a, miR-1, and miR-200b. (**d**) Electropherograms (*top*) and virtual gel images (*bottom*) of FFPE samples of mouse liver (L1-4), pancreas (P1-4), and stomach (S1-4), which were generated using an Agilent 2100 Bioanalyzer. RNA 6000 Nano ladder, which includes 25 nt, 200 nt, 500 nt, 1000 nt, 2000 nt, and 4000 nt markers, is shown alongside (*bottom left*). RNA is fragmented in all of the FFPE samples.

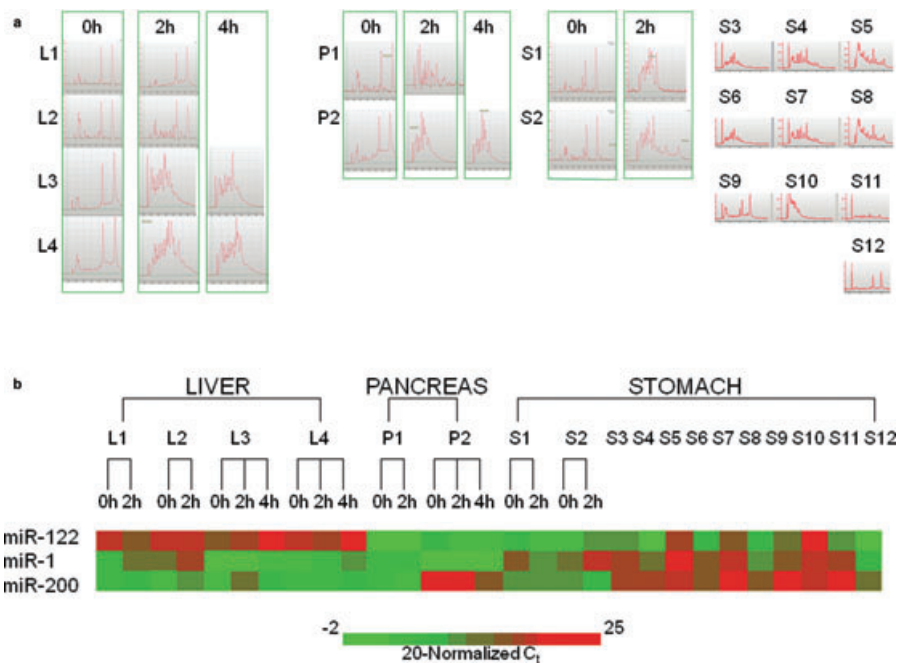


**Figure 2** (**a**) RNA integrity of clinical samples. Electropherograms were generated using an Agilent 2100 Bioanalyzer. L1-4, P1-2, and S1-2 represent liver, pancreas, and stomach tissue samples resected from patients, respectively. Each tissue sample was subjected to RNA isolation at flash-frozen state (0 h) and after 2 h- and 4 h-incubation at room temperature (2 h and 4 h). S3-12 endoscopic biopsy tissue samples from gastric cancer patients previously underwent a freeze-thaw cycle[10] and therefore demonstrate various degrees of RNA degradation. The degradation of ribosomal RNA is reflected by a shift towards shorter fragment sizes in electropherograms. (**b**) Quantitative reverse transcription polymerase chain reaction (QRTPCR) expression of tissue-specific microRNAs in clinical samples shown in (a). Heatmap generated from a pseudo-color image after median centering. Red and green indicate high and low normalized microRNA expression, respectively. RNA degradation-associated change in microRNA expression was small compared to expression difference associated with the tissue origin.

*vs.* 2.2 ± 0.3 (2-h)). In liver and stomach, average RIN was not significantly different between flash-frozen and 2-h incubation samples (Mean ± SD, 7.1 ± 2.7 (0-h) *vs.* 5.9 ± 1.9 (2-h) and 5.8 ± 3.2 (0-h) *vs.* 6.9 ± 1.4 (2-h), for liver and stomach, respectively). RNA was invariably fragmented in FFPE samples, as shown in Fig. 1d (Mean RIN ± SD,2.3 ± 0.1, 2.2 ± 0.1, and 2.1 ± 0.2, for liver, pancreas, and stomach, respectively).

According to the principal component analyses (PCA) based on the QRTPCR expression levels of the three

microRNAs, degraded RNA samples from normal mouse liver, pancreas, and stomach tissues tended to be clustered according to their tissue origin (Fig. 1b,c). The QRTPCR predictor based on miR-122a, miR-1, and miR-200b was then applied to predict the class label (liver, pancreas, or stomach) of two sets of degraded RNA samples from mice. Combined expression of the three microRNAs predicted the tissue origin of 2-h samples with an accuracy of 91.7%, while the accuracy of prediction for FFPE samples was 66.7% (Table 2). Hence, we conclude that miR-122a, miR-1, and miR-200b can reliably differentiate between mouse normal liver, pancreas, and stomach tissue, even when the RNA has been degraded by the extended storage at room temperature, but not in FFPE samples.

We moved on to evaluate the tissue specificity of these microRNAs in clinical samples before and after RNA degradation due to extended storage at room temperature. We isolated 19 total RNA samples from surgical specimens which were either flash-frozen ($n = 8$) or left at room temperature for 2–4 h longer than flash-frozen samples (2-h and 4-h, respectively) ($n = 11$). Most of the 2-h and 4-h tissue samples demonstrated the decrease in RIN (Table 3). QRTPCR expression of RNU6, which was used for normalization, was found to be relatively unchanged after prolonged incubation at room temperature (data not shown). QRTPCR expression levels of miR-1, miR-122a, and miR-200b were changed modestly after 2-h incubation at room temperature (Fig. 2b).

When we applied the 3-microRNA nearest centroid predictor to flash-frozen surgical specimens, the tissue origin was accurately predicted in 7 out of 8 flash-frozen surgical specimens (87.5%) (Table 3). Moreover, when the predictor was applied to 2-h and 4-h samples, the tissue origin was accurately predicted in all of the eleven RNA samples (Table 3). We also applied this 3-microRNA predictor to 10 endoscopic biopsy tissue samples that previously underwent a freeze-thaw cycle for another study.[10] As expected, RNA samples from these 10 tissue samples showed various degree of RNA degradation (Fig. 2a and Table 3). The prediction was accurate in 8 of 10 endoscopic biopsy samples (80%), and the prediction accuracy was not associated with the RIN. Overall, the tissue origin was accurately predicted in 90% of clinical samples (26/29) by the 3-microRNA predictor, suggesting that the magnitude of change in expression of individual microRNA after extended storage at room temperature or a freeze-thaw cycle is small relative to the expression differences across tissue types.

**Table 2** Prediction for the tissue origin of normal mouse tissue samples using QRTPCR for miR-122a, miR-1, and miR-200b

| | True class label | | | |
|---|---|---|---|---|
| | Liver | Pancreas | Stomach | Accuracy |
| After 2-h | 4/4 correct | 3/4 correct | 4/4 correct | 91.7% (11/12) |
| FFPE | 4/4 correct | 2/4 correct | 2/4 correct | 66.7% (8/12) |

FFPE, formalin-fixed, paraffin-embedded; QRTPCR, Quantitative Reverse Transcription Polymerase Chain Reaction.

## DISCUSSION

Our data demonstrate that 3-microRNA QRTPCR profiling of degraded RNA samples can differentiate between liver,

**Table 3** Prediction for the tissue origin of clinical tissue samples using QRTPCR for miR-122a, miR-1, and miR-200b

| ID | Patient Sex/Age | Diagnosis | Source tissue | RNA $RIN_{0h}$ | $RIN_{2h}$ | $RIN_{4h}$ | Accurate prediction |
|---|---|---|---|---|---|---|---|
| Surgical samples | | | | | | | |
| L1 | M/35 | HCC | Cancer | 6.8 | 6.6 | | 2/2 |
| L2 | M/35 | HCC | Adjacent liver | 6.5 | 4.4 | | 2/2 |
| L3 | M/55 | CBD cancer | Normal liver | 9.2 | 3.0 | 1.9 | 3/3 |
| L4 | F/48 | HCC | Adjacent liver | 7.7 | 4.1 | 1.8 | 3/3 |
| P1 | F/48 | Pancreas cancer | Cancer | 6.5 | 2.7 | | 2/2 |
| P2 | M/55 | CBD cancer | Normal pancreas | 7.4 | 1.8 | 1.9 | 2/3 (2 h, 4 h) |
| S1 | F/61 | Stomach cancer | Cancer | 6.0 | 2.5 | | 1/1 |
| S2 | F/65 | Stomach cancer | Cancer | 7.3 | 2.1 | | 1/1 |
| Biopsy samples (previously thawed and frozen) | | | | | | | |
| S3 | M/51 | Stomach cancer | Cancer | 2.2 | | | 1/1 |
| S4 | F/73 | Stomach cancer | Cancer | 4.2 | | | 1/1 |
| S5 | F/56 | Stomach cancer | Cancer | 3.2 | | | 1/1 |
| S6 | M/60 | Stomach cancer | Cancer | 5.5 | | | 1/1 |
| S7 | F/70 | Stomach cancer | Cancer | 4.5 | | | 1/1 |
| S8 | M/54 | Stomach cancer | Cancer | 6.3 | | | 1/1 |
| S9 | M/81 | Stomach cancer | Cancer | 7.3 | | | 1/1 |
| S10 | F/40 | Stomach cancer | Cancer | 2.3 | | | 0/1 |
| S11 | M/46 | Stomach cancer | Cancer | 2.0 | | | 1/1 |
| S12 | F/75 | Stomach cancer | Cancer | 8.5 | | | 0/1 |

0 h, flash-frozen; CBD, Common Bile Duct (distal); QRTPCR, Quantitative Reverse Transcription Polymerase Chain Reaction; RIN, RNA Integrity Number.

pancreas, and stomach tissue samples. Jung *et al.* reported robust stability of microRNAs in RNA samples degraded by heat (80°C).[4] According to Ibberson *et al.,* liver and duodenum samples from the same mouse showed distinct, tissue-specific microRNA profiles even after being incubated on ice for up to 4 h, although expression of individual microRNA is compromised by RNA degradation.[3] Our study confirms and extends these preclinical experimental data onto clinical samples. Combined expression of miR-1, miR-122a, and miR-200b, a novel microRNA combination, was found to be useful for differentiating between liver, pancreas, and stomach tissue samples from patients. Although this small set of primary tumor data cannot be directly applicable to clinical practice, it suggests the feasibility of evolutionarily-conserved microRNA QRTPCR as a possible approach to the diagnosis of primary tissue origin of metastatic lesions, given the accurate prediction results and the reported strong correlation in microRNA expression profile between metastasis and primary tumors.[6] miR-122a is a liver-specific microRNA.[13] miR-200 family members are important in the epithelial-mesenchymal transition.[14] miR-200c, as well as miR-141, is expressed at significantly higher levels in non-hepatic epithelial tumors than primary liver cancers.[15] Functional roles for our three tissue-specific microRNAs in the development of foregut epithelium have been largely unexplored.

This proof-of-principle study suggests that RNA degradation due to extended storage at room temperature or a freeze-thaw cycle may not affect the ability of miR-122a, miR-1, and miR-200b to differentiate between liver, pancreas, and stomach tissue samples. Changes in QRTPCR expression levels of miR-122a, miR-1, and miR-200b with the extended storage at room temperature, which mimics the typical clinical situations that lead to RNA degradation, are found to be small compared to the expression difference associated with the tissue origin. Relatively small number of clinical samples is a limitation of this analysis, but consistent mouse data supports our conclusion that RNA degradation due to extended storage at room temperature does not affect the predictive power of the tissue-specific microRNA profile.

## ACKNOWLEDGMENTS

The research was supported by the National Cancer Center Grant 0910570 and by Converging Research Center Program through the Ministry of Education, Science and Technology (2010K001121).

The authors thank Drs. Tinghu Qiu and Jeffrey E. Green at NCI.

## REFERENCES

1 Iorio MV, Croce CM. MicroRNAs in cancer: small molecules with a huge impact. *J Clin Oncol* 2009; **27**: 5848–56.
2 Shigoka M, Tsuchida A, Matsudo T *et al.* Deregulation of miR-92a expression is implicated in hepatocellular carcinoma development. *Pathol Int* 2010; **60**: 351–7.
3 Ibberson D, Benes V, Muckenthaler MU, Castoldi M. RNA degradation compromises the reliability of microRNA expression profiling. *BMC Biotechnol* 2009; **9**: 102–10.
4 Jung M, Schaefer A, Steiner I *et al.* Robust microRNA stability in degraded RNA preparations from human tissue and cell samples. *Clin Chem* 2010; **56**: 998–1006.
5 Xi Y, Nakajima G, Gavin E *et al.* Systematic analysis of microRNA expression of RNA extracted from fresh frozen and formalin-fixed paraffin-embedded samples. *RNA* 2007; **13**: 1668–74.
6 Rosenfeld N, Aharonov R, Meiri E *et al.* MicroRNAs accurately identify cancer tissue origin. *Nat Biotechnol* 2008; **26**: 462–9.
7 Lu J, Getz G, Miska EA *et al.* MicroRNA expression profiles classify human cancers. *Nature* 2005; **435**: 834–8.
8 Zaret KS, Grompe M. Generation and regeneration of cells of the liver and pancreas. *Science* 2008; **322**: 1490–94.
9 Becker C, Hammerle-Fickinger A, Riedmaier I, Pfaffl MW. mRNA and microRNA quality control for RT-qPCR analysis. *Methods* 2010; **50**: 237–43.
10 Kim HK, Reyzer ML, Choi IJ *et al.* Gastric cancer-specific protein profile identified using endoscopic biopsy samples via MALDI mass spectrometry. *J Proteome Res* 2010; **9**: 4123–30.
11 Schroeder A, Mueller O, Stocker S *et al.* The RIN: an RNA integrity number for assigning integrity values to RNA measurements. *BMC Mol Biol* 2006; **7**: 3–16.
12 Simon R, Lam A, Li MC *et al.* Analysis of gene expression data using BRB-Array Tools. *Cancer Informatics* 2007; **2**: 11–17.
13 Landgraf P, Rusu M, Sheridan R *et al.* A mammalian microRNA expression atlas based on small RNA library sequencing. *Cell* 2007; **129**: 1401–14.
14 Mongroo PS, Rustgi AK. The role of the miR-200 family in epithelial-mesenchymal transition. *Cancer Biol Ther* 2010; **10**: 219–22.
15 Barshack I, Meiri E, Rosenwald S *et al.* Differential diagnosis of hepatocellular carcinoma from metastatic tumors in the liver using microRNA expression. *Int J Biochem Cell Biol* 2010; **42**: 1355–62.